J|A|C|S ARTICLES

Published on Web 07/23/2010

Reactivity of [1],[1]Disilamolybdenocenophane toward Zerovalent Platinum Complexes

Holger Braunschweig,* Peter Brenner, Manuela Gross, and Krzysztof Radacki

Institut für Anorganische Chemie, Julius-Maximilians-Universität Würzburg, Am Hubland, D-97074 Würzburg, Germany

Received June 7, 2010; E-mail: h.braunschweig@mail.uni-wuerzburg.de

Abstract: The results of studies of the reactivity of strained [1],[1]disilamolybdenocenophane toward zerovalent platinum complexes are reported. Whereas $[Pt(PEt_3)_3]$ underwent clean insertion into both $Si-C_{ispo}$ bonds of the twofold-bridged molybdenocene, the reaction with the tricyclohexylphosphine analogue is considerably more complex. Thus, treatment of the molybdenum compound with 2 equiv of $[Pt(PCy_3)_2]$ results in a trinuclear cluster. To gain insight into the mechanistic aspects, the reaction was performed in a 1:1 stoichiometry. Multinuclear NMR spectroscopy revealed the presence of different species in solution. Two constitutional isomers were identified by X-ray diffraction analyses, one presumably depicting an intermediate in the formation of the trinuclear cluster. The predominant isomer in solution was identified as the product of C−H oxidative addition to the platinum phosphine fragment. Its solid-state structure displays an unusual coordination mode of platinum, and structural parameters suggest the formulation as the σ-complex of a Mo−Si bond.

Introduction

Platinum group metals play an important role in organic syntheses, providing access to various functionalized substrates, for instance, by catalyzing cross-coupling reactions[1] and addition of element−element bonds to unsaturated organic reagents.[2]

Thus, facile metal-mediated activation of the E−E bond of [2]metalloarenophanes enables transfer of organometallic moieties to unsaturated substrates under both stoichiometric and catalytic conditions.[3] Furthermore, ring-opening polymerization (ROP) of strained [1]metalloarenophanes catalyzed by late transition metals provides access to organometallic polymers, which display promising applications in materials science.[3j,4] Hence, due to the versatile applications and their unique structure, bonding, and reactivity patterns, *ansa*-complexes have attracted increasing interest in recent decades.

Scheme 1. Synthesis of [1],[1]Disilamolybdenocenophane **2**

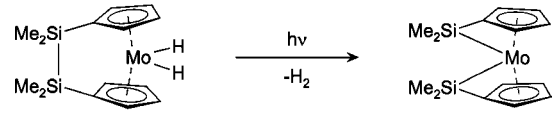

1 **2**

Recently, we accomplished the first intramolecular insertion of a metal center into the bridging moiety of a [2]metallocenophane. Photolysis of [2]disilamolybdenocenophane dihydride (**1**) induces reductive elimination of dihydrogen and subsequent oxidative addition of the Si−Si bond to the metal center (Scheme 1).[5] Subsequently, we investigated the electronic structure of the twofold-bridged complex **2** by theoretical

(1) See, for instance: (a) Miyaura, N.; Suzuki, A. *Chem. Rev.* **1995**, *95*, 2457–2483. (b) Stille, J. K. *Angew. Chem.* **1986**, *98*, 504−519; *Angew. Chem., Int. Ed. Engl.* **1986**, *25*, 508−524. (c) Stille, J. K. *Pure Appl. Chem.* **1985**, *57*, 1771–1780. (d) Hartwig, J. F. *Nature* **2008**, *455*, 314–322. (e) Mkhalid, I. A. I.; Barnard, J. H.; Marder, T. B.; Murphy, J. M.; Hartwig, J. F. *Chem. Rev.* **2010**, *110*, 890–931.

(2) See, for instance: (a) Marder, T. B.; Norman, N. C. *Top. Catal.* **1998**, *5*, 63–73. (b) Ishiyama, T.; Matsuda, N.; Miyaura, N.; Suzuki, A. *J. Am. Chem. Soc.* **1993**, *115*, 11018–11019. (c) Beletskaya, I.; Moberg, C. *Chem. Rev.* **1999**, *99*, 3435–3461. (d) Beletskaya, I.; Moberg, C. *Chem. Rev.* **2006**, *106*, 2320–2354. (e) Ishiyama, T.; Miyaura, N. *J. Organomet. Chem.* **2000**, *611*, 392–402.

(3) (a) Braunschweig, H.; Lutz, M.; Radacki, K.; Schaumloeffel, A.; Seeler, F.; Unkelbach, C. *Organometallics* **2006**, *25*, 4433–4435. (b) Braunschweig, H.; Lutz, M.; Radacki, K. *Angew. Chem.* **2005**, *117*, 5792−5796; *Angew. Chem., Int. Ed.* **2005**, *44*, 5647−5651. (c) Finckh, W.; Tang, B. Z.; Lough, A.; Manners, I. *Organometallics* **1992**, *11*, 2904–2911. (d) Herberhold, M.; Steffl, U.; Milius, W.; Wrackmeyer, B. *Angew. Chem.* **1997**, *109*, 1545−1546; *Angew. Chem., Int. Ed. Engl.* **1997**, *36*, 1508−1510. (e) Herberhold, M.; Steffl, U.; Wrackmeyer, B. *J. Organomet. Chem.* **1999**, *577*, 76–81. (f) Braunschweig, H.; Kupfer, T. *Organometallics* **2007**, *26*, 4634–4638. (g) Braunschweig, H.; Kupfer, T. *J. Am. Chem. Soc.* **2008**, *130*, 4242–4243. (h) Braunschweig, H.; Kaupp, M.; Adams, C. J.; Kupfer, T.; Radacki, K.; Schinzel, S. *J. Am. Chem. Soc.* **2008**, *130*, 11376–11393. (i) Braunschweig, H.; Kupfer, T.; Lutz, M.; Radacki, K.; Seeler, F.; Sigritz, R. *Angew. Chem.*, **2006**, *118*, 8217−8220; *Angew. Chem., Int. Ed.* **2006**, *45*, 8048−8051. (j) Braunschweig, H.; Kupfer, T. *Acc. Chem. Res.* **2010**, *43*, 455–465.

(4) (a) Bellas, V.; Rehahn, M. *Angew. Chem.* **2007**, *119*, 5174−5197; *Angew. Chem., Int. Ed. Engl.* **2007**, *46*, 5082−5104. (b) Temple, K.; Jaekle, F.; Sheridan, J. B.; Manners, I. *J. Am. Chem. Soc.* **2001**, *123*, 1355–1364. (c) Nguyen, P.; Gomez-Elipe, P.; Manners, I. *Chem. Rev.* **1999**, *99*, 1515–1548. (d) Manners, I. *Can. J. Chem.* **1998**, *76*, 371–381. (e) Tamm, M.; Kunst, A.; Bannenberg, T.; Randoll, S.; Jones, P. G. *Organometallics* **2007**, *26*, 417–424. (f) Tamm, M.; Kunst, A.; Herdtweck, E. *Chem. Commun.* **2005**, 1729–1731. (g) Bartole-Scott, A.; Braunschweig, H.; Kupfer, T.; Lutz, M.; Manners, I.; Nguyen, T.; Radacki, K.; Seeler, F. *Chem.—Eur. J.* **2006**, *12*, 1266–1273. (h) Temple, K.; Lough, A. J.; Sheridan, J. B.; Manners, I. *J. Chem. Soc., Dalton Trans.* **1998**, 2799–2806. (i) Sheridan, J. B.; Lough, A. J.; Manners, I. *Organometallics* **1996**, *15*, 2195–2197.

(5) Braunschweig, H.; Gross, M.; Radacki, K.; Rothgaengel, C. *Angew. Chem.* **2008**, *120*, 10127−10129; *Angew. Chem., Int. Ed.* **2008**, *47*, 9979−9981.

Scheme 2. Synthesis of **3**

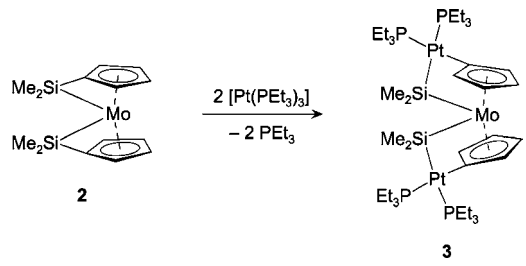

methods, revealing a strained $\kappa Si{:}\eta^5$ bonding mode, and studied its reactivity toward unsaturated organic substrates.[6]

Compound **2** reacts separately with 2-butyne and *trans*-azobenzene, affording [2]metallocenophanes with side-on coordinated substrates, while treatment with *tert*-butylisonitrile results in an unusual Fischer-type carbene *ansa*-complex.[6] We now turn our attention to the reactivity of **2** toward zerovalent platinum complexes.

Results and Discussion

Since a rich insertion chemistry of triethylphosphine-substituted zerovalent platinum fragments into bridging moieties of *ansa*-complexes has already been reported,[4e−i] we first attempted the reaction of [1],[1]molybdenocenophane **2** with 2 equiv of $[Pt(PEt_3)_3]$ in benzene, which resulted in an orange-colored reaction mixture. Monitoring the reaction by ^{31}P NMR spectroscopy revealed liberation of triethylphosphine and formation of a new phosphorus-containing species. The ^{31}P NMR spectrum displays two doublets at 16.7 and 10.8 ppm ($^2J_{P,P}$ = 3.7 Hz) flanked by ^{195}Pt satellites with coupling constants of 2896 and 892 Hz, respectively, which is indicative of a *cis*-coordinated bis(phosphine)platinum complex. Due to the strong *trans* influence of the silyl ligands, the coupling constant for the latter is significantly lower. Hence, oxidative addition of both $Si-C_{ipso}$ bonds to platinum fragments is assumed (Scheme 2), resembling the reactivity of strained [1]silametalloarenophanes toward zerovalent platinum complexes but yielding a rare example of a [2],[2]metallocenophane.[4e−i] Isolation of compound **3** yielded an air- and moisture-sensitive yellow solid in 57% yield, which decomposes in solution within several days.

To confirm the proposed structure, single crystals suitable for X-ray diffraction analysis were grown from Et_2O at −35 °C. In the solid state, **3** adopts C_2 symmetry (Figure 1), consistent with the NMR spectroscopic data in solution. Both the Mo−Si (2.5552(17) Å) and the Pt−Si (2.3977(16) Å) bond lengths are in the range typical for the corresponding metal−silicon single bonds.[7] A long Mo−Pt distance (3.8869(14) Å) and an obtuse Mo−Si−Pt angle (103.35(5)°) indicate a bonding situation at silicon best described as a bismetalated silane complex, consistent with the chemical shift of the ^{29}Si NMR resonance at −27.2 ppm.[7,8] In addition, the platinum atom is coordinated almost planar, with a sum of angles of 360.53°. However, probably because of the constrained geometry, the silyl ligands cannot adopt the position that would be expected for square planar coordination of platinum ($C_{ipso}-Pt-Si$ 69.02(14)°, Si−Pt−P2 98.38(6)°, P1−Pt−P2 106.36(6)°, $P1-Pt-C_{ipso}$ 86.77(14)°). Although the silyl ligand is not coordinated perfectly in the position *trans* to P1 (P1−Pt−Si 154.48(5)°), its strong *trans* influence is reflected by a significantly elongated Pt−P bond (Pt−P1 2.3783(16) Å, Pt−P2 2.2604(17) Å).[4e−i]

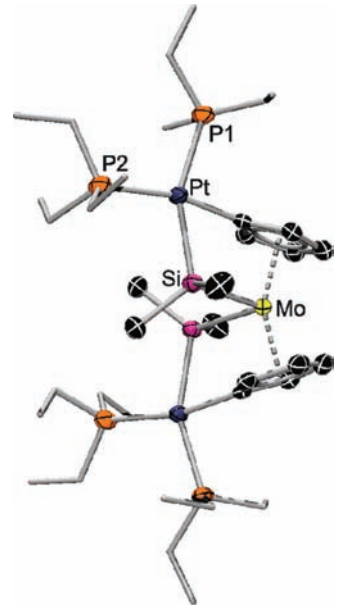

Figure 1. Molecular structure of **3**. Thermal ellipsoids are shown at the 50% probability level. All hydrogen atoms and the ellipsoids as well as the disorder of the ethyl groups are omitted for clarity. Selected bond lengths [Å] and angles [°]: Mo−Si 2.5552(17), Pt−Si 2.3977(16), $Pt-C_{ipso}$ 2.0476(55), Pt−P1 2.3783(16), Pt−P2 2.2604(17), Mo−Si−Pt 103.35(5), $C_{ipso}-Pt-Si$ 69.02(14), $C_{ipso}-Pt-P1$ 86.77(14), P1−Pt−P2 106.36(6), P2−Pt−Si 98.38(6), C−Si−C 101.73(33).

On the basis of this facile oxidative addition of both $Si-C_{ipso}$ bonds of **2** to $[Pt(PEt_3)_2]$ fragments, we focused our reactivity studies on the bulkier $[Pt(PCy_3)_2]$ complex. Monitoring the reaction of **2** with 2 equiv of $[Pt(PCy_3)_2]$ by ^{31}P NMR spectroscopy revealed liberation of 2 equiv of tricyclohexylphosphine and formation of a new compound (**4**), exhibiting two nonequivalent $[Pt(PCy_3)]$ moieties [70.8 ($^1J_{P,Pt}$ = 4390 Hz, $^2J_{P,Pt}$ = 134 Hz) and 67.7 ($^1J_{P,Pt}$ = 3580 Hz, $^2J_{P,Pt}$ = 165 Hz) ppm]. A small coupling constant of $^3J_{P,P}$ = 9.8 Hz suggests the presence of a bent P−Pt−Pt−P moiety.[9] The ^{29}Si NMR spectrum features two distinct resonances, one at −0.7 ppm, indicative of a metal-bound silicon nucleus,[4i,10] and one very broad signal shifted to low field (167.2 ppm),[11] which is in agreement with previously reported downfield-shifted ^{29}Si NMR resonances of dinuclear bridged silylene complexes.[7,8,12] However, due to the poor solubility of **4** in benzene and tetrahydrofuran and the lack of stability in dichloromethane, no silicon platinum satellites were detected. After workup, a highly air- and moisture-sensitive dark-red solid was isolated in 69% yield. To elucidate the structure of **4**, single crystals were grown from

(6) Arnold, T.; Braunschweig, H.; Gross, M.; Kaupp, M.; Mueller, R.; Radacki, K. *Chem.—Eur. J.* **2010**, *16*, 3014–3020.
(7) Corey, J. Y.; Braddock-Wilking, J. *Chem. Rev.* **1999**, *99*, 175–292.
(8) Ogino, H.; Tobita, H. *Adv. Organomet. Chem.* **1998**, *42*, 223–290.
(9) Braunstein, P.; De Meric de Bellefon, C.; Bouaoud, S. E.; Grandjean, D.; Halet, J. F.; Saillard, J. Y. *J. Am. Chem. Soc.* **1991**, *113*, 5282–5292.
(10) (a) Shimada, S.; Li, Y. H.; Rao, M. L. N.; Tanaka, M. *Organometallics* **2006**, *25*, 3796–3798. (b) Yamashita, H.; Tanaka, M.; Goto, M. *Organometallics* **1997**, *16*, 4696–4704.
(11) The very broad resonance was confirmed by $^{29}Si,^1H$ NMR COSY.
(12) (a) Zhang, Y.; Cervantes-Lee, F.; Pannell, K. H. *Organometallics* **2003**, *22*, 2517–2524. (b) Pannell, K. H.; Sharma, H. K.; Kapoor, R. N.; Cervantes-Lee, F. *J. Am. Chem. Soc.* **1997**, *119*, 9315–9316. (c) Gadek, A.; Kochel, A.; Szymanska-Buzar, T. *Organometallics* **2003**, *22*, 4869–4872.

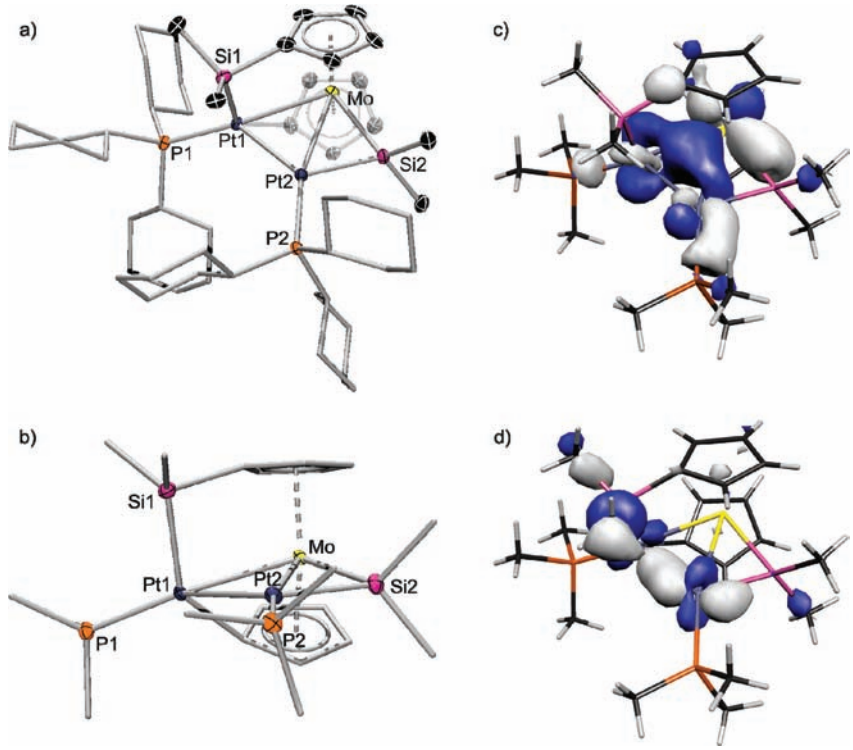

Figure 2. (a) Molecular structure of **4**. Thermal ellipsoids are shown at the 50% probability level. The second molecule of the asymmetric unit as well as the solvent molecule, the hydrogen atoms, and the ellipsoids of the cyclohexyl groups are omitted for clarity. Selected bond lengths [Å] and angles [°]: Mo−Pt1 2.7624(6), Mo−Pt2 2.8116(6), Pt1−Pt2 2.8657(3), Pt1−Si1 2.3211(17), Mo−Si2 2.5231(19), Pt2−Si2 2.2643(18), Pt1−C_{ipso} 2.0644(63), Si1−C_{ipso} 1.8895(69), Pt1−P1 2.2452(17), Pt2−P2 2.2405(17), Mo−Si2−Pt2 71.70(5), Si2−Pt2−Mo 58.43(5), Pt2−Mo−Si2 49.87(4), C−Si2−C 98.72(33), Pt1−Mo−Pt2 61.87(1), Pt2−Pt1−Mo 59.91(1), Mo−Pt2−Pt1 58.22(1), C_{ipso}−Pt1−Mo 53.68(16), C_{ipso}−Pt1−P1 108.62(17), P1−Pt1−Pt2−P2 −16.89(9); Mo′−Pt1′ 2.7716(6), Mo′−Pt2′ 2.8240(6), Pt1′−Pt2′ 2.8554(4), Pt1′−Si1′ 2.3032(18), Mo′−Si2′ 2.5178(19), Pt2′−Si2′ 2.2657(17), Pt1′−C_{ipso}′ 2.0690(59), Si1′−C_{ipso}′ 1.8863(71), Pt1′−P1′ 2.2428(16), Pt2′−P2′ 2.2365(16), Mo′−Si2′−Pt2′ 72.15(5), Si2′−Pt2′−Mo′ 58.06(5), Pt2′−Mo′−Si2′ 49.79(4), C′−Si2′−C′ 100.14(33), Pt1′−Mo′−Pt2′ 61.36(1), Pt2′−Pt1′−Mo′ 60.23(1), Mo′−Pt2′−Pt1′ 58.42(1), C_{ipso}′−Pt1′−Mo′ 53.47(18), C_{ipso}′−Pt1′−P1′ 115.43(18), P1′−Pt1′−Pt2′−P2′ −1.40(8). (b) Alternative view on the simplified molecular structure of **4**. (c) HOMO−2 of **4′**. (d) HOMO−14 of **4′**.

Scheme 3. Synthesis of **4**

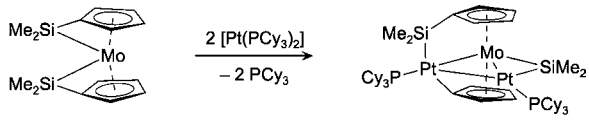

2 **4**

toluene at −35 °C. The results of an X-ray diffraction study (Figure 2a,b) are in agreement with the NMR spectroscopic data. Hence, the reaction product is identified as the trinuclear cluster **4** depicted in Scheme 3.

Two independent molecules of **4** are found in the asymmetric unit, for which the relevant structural parameters are almost identical, differing mainly in the orientation of the tricyclohexylphosphines of the bent P1−Pt1−Pt2−P2 moieties (torsion: −16.89(9) and −1.40(8)°, respectively). Thus, in the following we confine our discussion to one molecule.

The most remarkable structural feature of **4** is the $MoPt_2$ triangle, with one platinum atom incorporated into the bridging Pt1−Si1 moiety, which connects both cyclopentadienyl rings of the molybdenocene unit. Furthermore, the triangle is capped by a bridging silylene ligand at the opposite Mo−Pt2 side. The Pt1−Pt2 bond distance of 2.8657(3) Å is slightly longer than the Pt−Pt bond lengths found for other trinuclear cluster compounds (2.605−2.748 Å),[13] whereas the Mo−Pt distances (Mo−Pt1 2.7624(6) Å, Mo−Pt2 2.8116(6) Å) are in the range of previously reported Mo−Pt bonds observed in heterometallic clusters.[9,13] The symmetrically bridging Si2 atom (sum of angles $MoSiMe_2$ 344.49°; sum of angles $PtSiMe_2$ 340.31°) exhibits an Mo−Si2−Pt2 angle of 71.70(5)°, characteristic of bridged silylene complexes with short M−M′ distances, which is also consistent with the pronounced downfield shift in the ^{29}Si NMR spectrum.[8]

To gain insight into the bonding situation of **4**, DFT calculations at the B3LYP level of theory were performed on the slightly simplified model compound **4′**, in which the tricyclohexylphosphine ligands were replaced by trimethylphosphine. The Wiberg bond index of the Pt1−Pt2 bond (0.08) implies a minor degree of contribution of covalency, although the computed canonical Kohn−Sham molecular orbital (MO) [HOMO−14] provides evidence for an interaction of the platinum atoms (Figure 2d). Further inspection of the MOs revealed a strongly delocalized electronic structure of the $MoPt_2$ core (Figure 2c), indicating a more complex bonding situation, which renders an appropriate description of complex **4** via simple Lewis-type formulas quite difficult.

To investigate the mechanistic aspects of the formation of the trinuclear metal cluster **4**, we reacted **2** with $[Pt(PCy_3)_2]$ in a 1:1 stoichiometry. Addition of a toluene solution of the platinum complex to a toluene solution of **2** resulted in an immediate color change of the reaction mixture to green. Monitoring the reaction by ^{31}P NMR spectroscopy revealed

(13) (a) Braunstein, P.; Jud, J. M.; Dusausoy, Y.; Fischer, J. *Organometallics* **1983**, *2*, 180–183. (b) Archambault, C.; Bender, R.; Braunstein, P.; Bouaoud, S. E.; Rouag, D.; Golhen, S.; Ouahab, L. *Chem. Commun.* **2001**, 849–850.

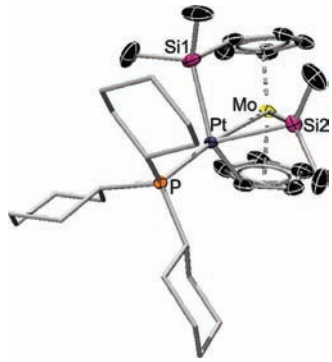

Figure 3. Molecular structure of **5**. Thermal ellipsoids are shown at the 50% probability level. The hydrogen atoms and the ellipsoids of the cyclohexyl ligands are omitted for clarity. Selected bond lengths [Å] and angles [°]: Mo−Pt 2.6821(3), Mo−Si2 2.5135(9), Pt−Si1 2.3450(8), Pt−Si2 2.3707(8), Pt−C 2.1556(28), Pt−P 2.2846(7), Mo−Si2−Pt 66.54(2), Si2−Pt−Mo 59.28(2), Pt−Mo−Si2 54.18(2), C−Si2−C 98.52(19), C_{ipso}−Pt−Mo 53.79(7), C_{ipso}−Pt−P 117.17(7), P−Pt−Si1 108.64(3), Si1−Pt−Mo 79.36(2), C−Si1−C 107.5(2).

liberation of tricyclohexylphosphine and formation of three new phosphorus-containing compounds, with resonances at 82.4, 74.6, and 52.7 ppm, respectively. Within 6 h the color of the solution changed to red, and complete consumption of [Pt-$(PCy_3)_2$] was observed via ^{31}P NMR spectroscopy. The species with a resonance at 52.7 ppm was identified as the predominant product. The ^{29}Si NMR spectrum displays two resonances, indicating two nonequivalent silicon nuclei. One signal was detected at 0.4 ppm ($^2J_{Si,P}$ = 52 Hz), suggesting a metal-bound silicon atom (**4**: −0.7 ppm), while the other chemical shift, 86.6 ppm, resembles that observed for the starting compound **2** (91.0 ppm).[5] Furthermore, the ^{1}H NMR spectrum displays a signal shifted to high field (−6.25 ppm) that features ^{31}P coupling (13 Hz) and ^{195}Pt satellites (576 Hz), which is indicative for a platinum hydride complex.[14] Because of difficulties associated with the removal of free tricyclohexylphosphine, the product was isolated only in low yields (23%) as a red solid. The elemental composition of this solid was determined by elemental analysis, which is in agreement with the formation of a 1:1 adduct of **2** and a [Pt(PCy_3)] fragment. Nevertheless, NMR spectroscopy of the solid confirmed the presence of a second species in solution [^{31}P NMR 74.6 ppm; ^{1}H NMR (broad resonances) 4.51, 3.90, 0.67 ppm (additional signals were overlaid by the resonances of PCy_3 referred to the predominant species)]. Within the accuracy of measurement, a ratio of 3:1 was constantly observed for the two species. Addition of a further equivalent of [Pt$(PCy_3)_2$] to a mixture of this composition was accompanied by the liberation of 1 equiv of PCy_3 and clean formation of the trinuclear complex **4**. These results suggest the presence of at least two interconvertable constitutional isomers in solution. However, our attempts to confirm this by variable-temperature (VT) NMR experiments failed due to thermal instability.

Single crystals suitable for X-ray diffraction analysis were obtained from pentane at −35 °C. The crystal structure of **5** (Figure 3) is in fairly good agreement with the bulk composition of the isolated red solid as determined by elemental analysis. However, the molecular structure of **5** is clearly not consistent with the solution NMR data, as it does not explain the observation of a hydride resonance in the ^{1}H NMR spectrum. However, only a few single crystals of **5** were isolated reproducibly; thus, full spectroscopic data could not be obtained.

The molecular structure of **5** displays a Pt−Si1 moiety, which connects both cyclopentadienyl rings, and thus resembles the structural motif of **4**. However, a significantly elongated Pt−Si2 distance (**5**: Pt−Si2 2.3707(8) Å) indicates a different bonding mode for the Si2 moiety in **5**, compared to the symmetrically bridging silylene ligand bound to the $MoPt_2$ triangle in **4** (**4**: Pt2−Si2 2.2643(18) Å). Furthermore, a shortened Mo−Pt bond distance (**5**, Mo−Pt 2.6821(3) Å; **4**, Mo−Pt2 2.8116(6) Å) is observed, whereas the Mo−Si2 bond lengths of the two compounds (**5**, 2.5135(9) Å; **4**, 2.5231(19) Å) are almost identical. The sum of angles at Si2 in **5** indicates planarity of the $MoSiMe_2$ moiety (357.20°), matching the structural features of metal-coordinated silicon in a low coordination number[15] even better than those of other asymmetrically heterodinuclear bridged silylene complexes (∼350°).[12b,16] The bonding mode of a previously described related platinum−iron silylene complex, [$(OC)_4FeSiR_2PtL_2$], was reported to be between two resonance forms, a platinum η^2-iron silylene complex and a bridged heterodinuclear silylene complex, although its molecular structure could not be determined by X-ray diffraction.[17] However, the planarity of the $MoSiR_2$ moiety resembles the geometry of semibridging borylene ligands. For instance, [$(Cy_3P)(OC)_3Mo(\mu$-CO)$\{\mu$-BN$(SiMe_3)_2\}$Pt(PCy_3)] exhibits an almost linear coordination of boron (153.2(4)°), ascribed to its lower coordination number.[18] Hence, on the basis of the geometrical parameters, we prefer the description of the Si2 moiety in **5** as a semibridging bonding mode, though the proposed structure could not be confirmed in solution by spectroscopic characterization. Despite that, formal insertion of a [Pt(PCy_3)] fragment into the Pt−Si2 bond of **5** can easily be considered as a key step in the formation of the trinuclear compound **4**. Hence, **5** presumably displays a constitutional isomer of the observed predominant species.

To elucidate the structure of the predominant constitutional isomer, further single crystals were grown by recrystallization of the isolated material from pentane at −35 °C. Indeed, X-ray diffraction of another batch of single crystals provided the solid-state structure of the platinum hydride complex **6**. The crystallographic data (Figure 4) unequivocally confirmed the presence of a hydrogen atom at platinum, which indicates the oxidative addition of a C−H bond of a cyclopentadienyl proton to platinum and therefore is in full agreement with the NMR data of the predominant species in solution (Scheme 4).

The most striking feature of the molecular structure of **6** is the planar, formally pentacoordinated platinum atom (sum of angles 360.11°). The long Si−H distance of 2.2235(295) Å rules out a platinum σ(Si−H) complex; however, it is still in the range of weak attractive interactions.[7,19] Deeper insight into the bonding situation of **6** requires a closer inspection

(14) (a) Paiaro, G.; Pandolfo, L.; Ganis, P.; Valle, G. *Organometallics* **1991**, *10*, 1527–1530. (b) Shaw, B. L.; Uttley, M. F. *J. Chem. Soc., Chem. Commun.* **1974**, 918–919.

(15) (a) Hirotsu, M.; Nunokawa, T.; Ueno, K. *Organometallics* **2006**, *25*, 1554–1556. (b) Feldman, J. D.; Mitchell, G. P.; Nolte, J. O.; Tilley, T. D. *Can. J. Chem.* **2003**, *81*, 1127–1136.

(16) Tanabe, M.; Osakada, K. *Inorg. Chim. Acta* **2003**, *350*, 201–208.

(17) Bodensieck, U.; Braunstein, P.; Deck, W.; Faure, T.; Knorr, M.; Stern, C. *Angew. Chem.* **1994**, *106*, 2561−2564; *Angew. Chem., Int. Ed. Engl.* **1994**, *33*, 2440−2442.

(18) (a) Braunschweig, H.; Radacki, K.; Uttinger, K. *Eur. J. Inorg. Chem.* **2007**, 4350–4356. (b) Braunschweig, H.; Radacki, K.; Rais, D.; Seeler, F. *Angew. Chem.* **2006**, *45*, 1066−1069; *Angew. Chem., Int. Ed.* **2006**, *45*, 1066−1069. (c) Braunschweig, H.; Whittell, G. R. *Chem.—Eur. J.* **2005**, *11*, 6128–6133.

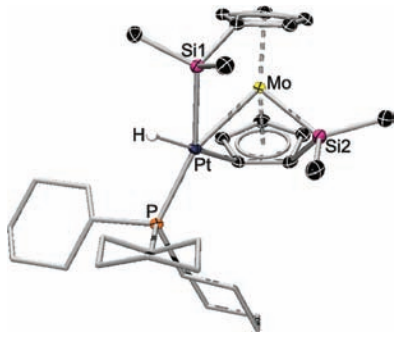

Figure 4. Molecular structure of **6**. Thermal ellipsoids are shown at the 50% probability level. All hydrogen atoms except that attached to Pt and the ellipsoids of the cyclohexyl ligands are omitted for clarity. Selected bond lengths [Å] and angles [°]: Mo−Pt 2.8336(3), Mo−Si2 2.4883(8), Pt−Si1 2.4151(7), Pt−C 2.0579(25), Pt−P 2.2875(7), Pt−H 1.6523(297), C_{ipso}−Pt−P 99.65(7), P−Pt−H 79.81(102), H−Pt−Si1 63.03(102), Si1−Pt−Mo 68.25(2), Mo−Pt−C_{ipso} 49.37(7), C−Si1−C 109.68(12), Mo−Si2−C_{ipso} 60.38(8), C−Si2−C 106.65(14).

Scheme 4. Synthesis of **6**

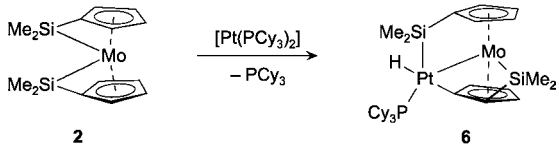

Table 1. Selected Bond Lengths [Å], Angles [°], and Wiberg Bond Indices from B3LYP DFT Calculations (WBI) of **2**, **6**, **5**, and **4**

	2	**6**	**5**	**4**
Mo−Si1	2.4866(4)	2.9647(8)	3.2204(9)	3.4394(19)
Mo−Si2	2.4915(4)	2.4883(8)	2.5135(9)	2.5231(19)
Mo−Pt		2.8336(3)	2.6821(3)	2.7624(6)
Mo−Pt2				2.8116(6)
Pt1−Si1		2.4151(7)	2.3450(8)	2.3211(17)
Pt−Si2			2.3707(8)	2.2643(18)
C_{ipso}−Si−Mo	61.15(4) 61.13(4)	50.19(7)	45.26(9)	41.18(18)
Si−Pt−Mo		68.25(2)	79.36(2)	84.68(5)
Si−Mo−Pt		49.17(2)	45.70(1)	42.22(3)
Mo−Si−Pt		62.59(2)	54.94(2)	53.10(4)
β (Si1−C_{ipso})[a]	48.7	32.11	23.05	16.07
β (Si2−C_{ipso})[a]	48.9	47.4		
β (Pt−C_{ipso})[a]		35.72	45.53	42.58
α[b]	20.48(7)	19.58(12)	30.01(14)	34.75(31)
δ[c]	159.4	156.2	150.3	146.8
WBI (Mo−Si1)	0.61	0.23		0.12
WBI (Mo−Si2)		0.6		0.71
WBI (Mo−Pt1)		0.23		0.24
WBI (Mo−Pt2)				0.23
WBI (Pt−Si1)		0.39		0.56
WBI (Pt−Si2)				0.64

[a] Deviation β: deviation of the E−C_{ipso} bond axis from the cyclopentadienyl ring plane. [b] Tilt angle α: angle between the cyclopentadienyl ring planes. [c] Deformation δ: X_{cp}−Mo−X_{cp} (X_{cp}: centroid of the cyclopentadienyl ring plane).

of its geometrical parameters and a detailed comparison with the starting complex **2** and the related compounds **4** and **5** (Table 1).

The Mo−Si1 distance of **6** (2.9647(8) Å) is significantly elongated compared to those found in the starting material **2** (2.4866(4) and 2.4915(4) Å, respectively). However, it is noticeably shorter than those of **4** (3.4394(19) Å) and **5** (3.2204(9) Å). Furthermore, the Pt−Si1 as well as the Mo−Pt

Scheme 5. Mesomeric Resonance Structures of Complex **6**

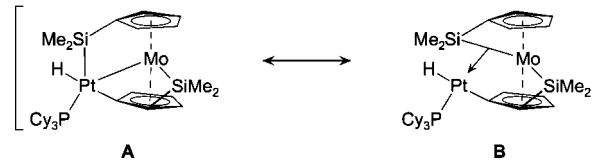

bond distances of **6** (2.4151(7) and 2.8336(3) Å, respectively) are significantly longer than those of **4** (2.3211(17) and 2.7624(6) Å, respectively) and **5** (2.3450(8) and 2.6821(3) Å, respectively). This trend is also reflected by the calculated Wiberg bond indices (Table 1). The weakening of the Mo−Si1 bond is accompanied by a gradual decrease of the C_{ipso}−Si1−Mo angles. Moreover, opening of the strained C_{ipso}−Si1−Mo moiety of **2** causes a change in the tilt angles and the deformation angles toward the values observed for nonbridged molybdenocenes ($\alpha = 34.2°$, $\delta = 151.5°$).[20] Thus, the solid-state structure of **6** most likely illustrates an earlier stage of the oxidative addition process involving the Mo−Si1 bond to platinum, as observed in **4** and **5**, respectively. Considering the centroid of the Mo−Si1 bond (X_{MoSi}) as one coordination site, platinum(II) displays an almost square-planar environment (H−Pt−P 79.8°, P−Pt−C_{ipso} 99.7°, C_{ipso}−Pt−X_{MoSi} 80.4°, X_{MoSi}−Pt−H 99.7°), which is expected for the heavier homologues of tetracoordinated d^8 late transition metals. Hence, σ-bond complexation (Scheme 5, **B**) is suggested, a common structural motif in organometallic chemistry, since various E−H[19,21] and, more recently, E−E σ-bond[22] complexes have been extensively studied.

Conclusion

In this paper we reported reactivity studies of the strained twofold-bridged [1],[1]molybdenocenophane toward zerovalent platinum complexes. Reaction of 2 equiv of [$Pt(PEt_3)_3$] with [(η^1:η^5-$Me_2SiC_5H_4)_2$Mo] (**2**) cleanly afforded the product of double Si−C_{ipso} bond oxidative addition to the metal fragments. Employing 2 equiv of the bulkier [$Pt(PCy_3)_2$], an unexpected reaction is observed yielding a trinuclear cluster. DFT calculations suggested a delocalized multicenter bonding. To gain insight into the mechanistic aspects of the formation of the trinuclear cluster **4**, the twofold-bridged molybdenocene **2** was reacted with equimolar amounts of [$Pt(PCy_3)_2$]. The constitutional isomers **5** and **6**, both representing adducts of **2** with one [$Pt(PCy_3)$] fragment, were identified by X-ray diffraction. **5** presumably depicts an intermediate in the formation of the

(19) (a) Perutz, R. N.; Sabo-Etienne, S. *Angew. Chem., Int. Ed.* **2007**, *46*, 2578–2592. (b) Lachaize, S.; Sabo-Etienne, S. *Eur. J. Inorg. Chem.* **2006**, 2115–2127. (c) Lin, Z. *Chem. Soc. Rev.* **2002**, *31*, 239–245. (d) Alcaraz, G.; Sabo-Etienne, S. *Coord. Chem. Rev.* **2008**, *252*, 2395–2409.

(20) (a) Schultz, A. J.; Stearley, K. L.; Williams, J. M.; Mink, R.; Stucky, G. D. *Inorg. Chem.* **1977**, *16*, 3303–3306. (b) Green, J. C. *Chem. Soc. Rev.* **1998**, *27*, 263–272.

(21) (a) Kubas, G. J. *Metal Dihydrogen and σ-Bond Complexes*; Kluwer Academic/Plenum Publishers: New York, 2001.

(22) (a) Chen, W.; Shimada, S.; Tanaka, M. *Science* **2002**, *295*, 308–310. (b) Crabtree, R. H. *Science* **2002**, *295*, 288–289. (c) Sherer, E. C.; Kinsinger, C. R.; Kormos, B. L.; Thompson, J. D.; Cramer, C. J. *Angew. Chem.* **2002**, *114*, 2033−2036; *Angew. Chem., Int. Ed.* **2002**, *41*, 1953−1956. (d) Aullon, G.; Lledos, A.; Alvarez, S. *Angew. Chem.* **2002**, *114*, 2036−2039; *Angew. Chem., Int. Ed.* **2002**, *41*, 1956−1959. (e) Nikonov, G. I. *Angew. Chem.* **2003**, *115*, 1375−1377; *Angew. Chem., Int. Ed.* **2003**, *42*, 1335−1337; (f) Brayshaw, S. K.; Sceats, E. L.; Green, J. C.; Weller, A. S. *Proc. Natl. Acad. Sci. U.S.A.* **2007**, *104*, 6921–6926.

trinuclear cluster **4**. However, the predominant isomer in solution, **6**, was identified as the product of C−H oxidative addition to the platinum phosphine fragment. Its solid-state structure displayed an unusual coordination mode of platinum, and the structural parameters suggest the formulation as a Mo−Si σ-complex to Pt.

Experimental Section

General Considerations. All manipulations were performed under an inert atmosphere of dry argon using either standard Schlenk-line or glovebox techniques. Toluene was purified and dried using an M. Braun solvent purification system and was stored over activated molecular sieves. Benzene, pentane, and diethyl ether were dried by distillation over potassium, sodium, and sodium/potassium alloy, respectively, and were stored over activated molecular sieves. [1],[1]Disilamolybdenocenophane was synthesized according to a literature procedure.[5] NMR spectra were recorded at 297 K on a Bruker Avance AV 500 NMR spectrometer and a Bruker Avance DMX 600 NMR spectrometer. Routine NMR measurements were performed on a Bruker Avance 200 NMR spectrometer. ^{1}H and ^{13}C{^{1}H} NMR spectra were referenced to external tetramethylsilane via the residual protio solvent (^{1}H) or the solvent itself (^{13}C). ^{31}P{^{1}H} NMR spectra were referenced to external 85% H_3PO_4, and ^{29}Si{^{1}H} NMR spectra were referenced to external $SiMe_4$. Chemical shifts (δ) are given in ppm. Elemental analyses were performed on an Elementar vario MICRO-cube elemental analyzer.

Synthesis of 3. An A J. Young NMR tube was filled with 60 mg (90 μmol) of [Pt(PEt_3)$_4$], and 1 equiv of triethylphosphine was removed in vacuo at 60 °C. The resulting red oil was dissolved in benzene (1 mL) and treated with 16 mg (45 μmol) of solid **2**. After 6 h at room temperature, all volatile materials in the orange solution were removed in vacuo. The residue was dissolved in Et_2O, and **3** was crystallized at −35 °C as yellow crystals (31 mg, 57%).

^{1}H NMR (500.13 MHz, C_6D_6): 4.94 (br s, 2H, C_5H_4), 4.40 (m, 2H, C_5H_4), 3.96 (m, 2H, C_5H_4), 3.93 (br s, 2H, C_5H_4), 1.79−1.69 (br m, 12H, CH_2, *Et*), 1.64−1.52 (br m, 12H, CH_2, *Et*), 1.18 (m, 6H, SiMe_2), 1.03−0.95 (br m, 36H, CH_3, *Et*), 0.94 (m, 6H, SiMe_2). ^{13}C NMR (125.76 MHz, C_6D_6): 93.41 (s, C_5H_4), 76.76 (s, C_5H_4), 76.48 (s, C_5H_4), 74.41 (s, C_5H_4), 65.66 (dd, C_{ipso}, $^{2}J_{C,P}$ = 97 Hz, $^{2}J_{C,P}$ = 10 Hz), 19.69 (m, CH_2, *Et*), 16.36 (m, CH_2, *Et*), 8.79 (m, SiMe_2), 8.69 (s, CH_3, *Et*), 8.32 (s, CH_3, *Et*), 6.71 (m, SiMe_2). ^{31}P NMR (202.46 MHz, C_6D_6): 16.7 (s, $^{1}J_{P,Pt}$ = 2896 Hz, $^{2}J_{P,C}$ = 97 Hz, PEt_3 *trans* to C_{ipso}), 10.8 (s, $^{1}J_{P,Pt}$ = 895 Hz, $^{2}J_{P,Si}$ = 102 Hz, PEt_3 *trans* to Si). ^{29}Si NMR (99.36 MHz, C_6D_6): −27.2 (d, $^{2}J_{Si,P}$ = 102 Hz, $^{1}J_{Si,Pt}$ = 700 Hz). Elemental analysis: calcd (%) for $C_{38}H_{80}Si_2MoPt_2P_4$ C 37.93, H 6.70; found C 37.89, H 6.63.

Synthesis of 4. A mixture of 50 mg (147 μmol) of **2** and 222 mg (294 μmol) of [Pt(PCy_3)$_2$] was dissolved in toluene (10 mL). After stirring for 18 h, a red solution was obtained. All volatiles of the reaction mixture were removed in vacuo, and the residue was washed five times with pentane to remove free PCy_3. A dark red solid of **4** was obtained in 69% yield (131 mg).

^{1}H NMR (600.13 MHz, C_6D_6): 5.92 (m, 1H, C_5H_4, $^{4}J_{H,Pt}$ = 22 Hz), 5.70 (m, 1H, C_5H_4); 5.08 (m, 1H, C_5H_4), 4.83 (m, 1H, C_5H_4), 4.43 (m, 1H, C_5H_4), 4.41 (m, 1H, C_5H_4), 3.88 (m, 1H, C_5H_4), 3.42 (m, 1H, C_5H_4), 2.36 (m, 3H, *Cy*), 2.10 (m, 3H, *Cy*), 2.01−1.24 (br m, 60H, *Cy*), 1.32 (s, 3H, Si(1)Me_2), 0.89 (s, 3H, Si(2)Me_2), 0.80 (s, 3H, Si(2)Me_2), 0.78 (s, 3H, Si(1)Me_2). ^{13}C NMR (150.92 MHz, C_6D_6): 181.84 (s, C_{ipso}Pt, $^{1}J_{C,Pt}$ = 663 Hz), 102.04 (s, C_5H_4), 88.34 (s, C_5H_4), 85.64 (s, C_5H_4), 83.64 (s, C_5H_4), 79.54 (s, C_5H_4), 79.35 (s, C_5H_4), 78.01 (s, C_{ipso}Si), 77.74 (s, C_5H_4), 76.89 (s, C_5H_4), 37.27 (d, C^1, *Cy*, $^{1}J_{C,P}$ = 22 Hz), 36.24 (br d, C^1, *Cy*), 31.82 (br s, $C^{3,5}$, *Cy*), 31.24 (br s, $C^{3,5}$, *Cy*), 30.97 (br s, $C^{3,5}$, *Cy*), 30.73 (br s, $C^{3,5}$, *Cy*), 28.28 (br d, $C^{2,6}$, *Cy*), 28.03 (br d, $C^{2,6}$, *Cy*), 27.96 (br d, $C^{2,6}$, *Cy*), 27.20 (s, C^4, *Cy*), 26.82 (s, C^4, *Cy*), 8.37 (s, Si(2)Me_2), 7.92 (s, Si(2)Me_2), 5.26 (s, Si(1)Me_2), 4.41 (br s, Si(1)Me_2); ^{31}P NMR (202.46 MHz, C_6D_6): 70.8 (d, PCy_3, $^{3}J_{P,P}$ = 9.8 Hz, $^{1}J_{P,Pt}$ = 4390 Hz, $^{2}J_{P,Pt}$ = 134 Hz), 67.7 (d, PCy_3, $^{3}J_{P,P}$ = 9.8 Hz, $^{1}J_{P,Pt}$ = 3580 Hz, $^{2}J_{P,Pt}$ = 165 Hz). ^{29}Si NMR (99.36 MHz, C_6D_6): 167.2 (br s, *Si*(2)), −0.7 (d, *Si*(1), $^{2}J_{Si,P}$ = 11 Hz). Elemental analysis: calcd (%) for $C_{50}H_{86}Si_2MoPt_2P_2$, C 46.50, H 6.71; found, C 46.47, H 6.70.

Synthesis of 6. A solution of 200 mg (264 μmol) of [Pt(PCy_3)$_2$] in toluene (30 mL) was added via cannula to a solution of 90 mg (264 μmol) of **2** in toluene (10 mL). The solution turned green, and after stirring for 18 h, all volatiles of the now red reaction mixture were removed in vacuo. The residue was recrystallized three times from pentane at −35 °C. A red solid of **6** was obtained in 23% yield (50 mg).

^{1}H NMR (500.13 MHz, C_6D_6): 5.70 (br, 1H, C_5H_3, $^{4}J_{H,Pt}$ = 20 Hz), 4.75 (br, 1H, C_5H_3), 4.72 (m, 1H, C_5H_3), 4.59 (br, 1H, C_5H_4), 4.56 (br, 1H, C_5H_4), 4.43 (br, 1H, C_5H_4), 4.17 (br, 1H, C_5H_4), 2.05−1.95 (br m, 9H, *Cy*), 1.75−1.69 (br m, 6H, *Cy*), 1.60−1.45 (br m, 9H, *Cy*), 1.19−1.12 (br m, 9H, *Cy*), 0.87 (s, 6H, Si(1)Me_2, $^{3}J_{H,Pt}$ = 26 Hz), 0.70 (s, 3H, Si(2)Me_2), 0.30 (s, 3H, Si(2)Me_2), −6.25 (d, 1H, Pt*H*, $^{2}J_{H,P}$ = 13 Hz, $^{2}J_{H,Pt}$ = 576 Hz). ^{13}C NMR (125.76 MHz, C_6D_6): 196.77 (s, C_{ipso}Pt), 97.22 (s, C_{ipso}Si(2)), 83.00 (s, C_5H_3), 82.82 (s, C_5H_4), 80.83 (s, C_5H_4), 80.56 (s, C_5H_3), 80.24 (s, C_5H_3), 79.89 (s, C_5H_4), 78.54 (s, C_5H_4), 66.90 (d, C_{ipso}Si(1), $^{3}J_{C,P}$ = 6 Hz), 38.03 (d, C^1, *Cy*, $^{1}J_{C,P}$ = 24 Hz), 30.65 (s, $C^{3,5}$, *Cy*), 27.54 (m, $C^{2,6}$, *Cy*), 26.74 (s, C^4, *Cy*), 5.11 (s, Si(2)Me_2), 4.80 (Si(1)Me_2), 4.54 (Si(1)Me_2), 0.66 (Si(2)Me_2). ^{31}P NMR (202.46 MHz, C_6D_6): 52.7 (s, PCy_3, $^{1}J_{P,Pt}$ = 2564 Hz, $^{2}J_{P,Si}$ = 52 Hz). ^{29}Si NMR (99.36 MHz, C_6D_6): 86.6 (s, *Si*(2)), 0.4 (d, *Si*(1), $^{2}J_{Si,P}$ = 52 Hz). Elemental analysis: calcd (%) for $C_{32}H_{53}Si_2MoPtP$, C 47.11, H 6.55; found, C 47.11, H 6.54.

Minor Species. ^{1}H NMR (500.13 MHz, C_6D_6): 4.51 (br s, 4 H), 3.90 (br s, 4 H), 0.67 (br s, 12 H). ^{31}P NMR (202.46 MHz, C_6D_6): 74.6 ppm. ^{13}C NMR and ^{29}Si NMR data could not be detected.

Crystal Structure Determination. The crystal data were collected with Mo Kα radiation and a CCD area detector on a Bruker D8 Apex I diffractometer with graphite monochromator (**3**) or on a Bruker X8 Apex II diffractometer with multilayer mirror monochromator (**4**−**6**). The structures were solved using direct methods, refined with the Shelx software package,[23] and expanded using Fourier techniques. All non-hydrogen atoms were refined anisotropically. All hydrogen atoms except the hydridic in **6** were assigned to idealized positions and were included in structure factors calculations. An electron residual peak (0.58 e$^-$) obtained from Fourier analysis indicates the presence of hydrogen *trans* to the carbon atom attached to platinum in **6**, and its position was freely refined.

Crystal Data for 3: M_r = 1203.20, yellow plate, 0.50 × 0.32 × 0.43 mm^3, tetragonal space group $P4_22_12$, a = 18.100(6) Å, b = 18.100(6) Å, c = 15.019(8) Å, α = 90.00°, β = 90.00°, γ = 90.00°, V = 4920(3) Å^3, Z = 4, ρ_{calcd} = 1.624 g·cm^{-3}, μ = 6.126 mm^{-1}, F(000) = 2376, T = 174(2) K, R_1 = 0.0354, wR_2 = 0.0702, 5850 independent reflections [$2\theta \leq 56.52°$] and 236 parameters.

Crystal Data for 4: $C_{103.5}H_{176}Mo_2P_4Pt_4Si_4$, M_r = 2628.92, orange plate, 0.06 × 0.04 × 0.015 mm^3, monoclinic space group $P2_1/c$, a = 38.232(2) Å, b = 13.6822(7) Å, c = 20.0104(11) Å, α = 90.00°, β = 96.374(3)°, γ = 90.00°, V = 10402.6(10) Å^3, Z = 4, ρ_{calcd} = 1.679 g·cm^{-3}, μ = 5.744 mm^{-1}, F(000) = 5236, T = 100(2) K, R_1 = 0.0737, wR_2 = 0.0896, 25 454 independent reflections [$2\theta \leq 56.7°$] and 1042 parameters.

Crystal Data for 5: $C_{32}H_{53}MoPPtSi_2$, M_r = 815.92, brown block, 0.2 × 0.15 × 0.12 mm^3, triclinic space group $P\bar{1}$, a = 9.4347(11) Å, b = 11.0663(12) Å, c = 16.4581(19) Å, α = 72.678(3)°, β = 85.306(4)°, γ = 78.765(3)°, V = 1608.5(3) Å^3, Z = 2, ρ_{calcd} = 1.685 g·cm^{-3}, μ = 4.878 mm^{-1}, F(000) = 816, T = 100(2) K, R_1 = 0.0221, wR_2 = 0.0531, 7920 independent reflections [$2\theta \leq 56.64°$] and 338 parameters.

Crystal Data for 6: $C_{32}H_{53}MoPPtSi_2$, M_r = 815.92, yellow block, 0.09 × 0.06 × 0.04 mm^3, triclinic space group $P\bar{1}$, a = 9.1633(12) Å, b = 11.3828(16) Å, c = 16.167(2) Å, α = 93.760(6)°, β =

(23) Sheldrick, G. M. *Acta Crystallogr.* **2008**, *A64*, 112–122.

99.869(5)°, $\gamma = 104.304(6)°$, $V = 1599.5(4)$ Å^3, $Z = 2$, $\rho_{calcd} = 1.694$ g·cm^{-3}, $\mu = 4.905$ mm^{-1}, $F(000) = 816$, $T = 100(2)$ K, $R_1 = 0.0229$, $wR_2 = 0.0525$, 7896 independent reflections [$2\theta \leq 56.68°$] and 341 parameters.

Crystallographic data have been deposited with the Cambridge Crystallographic Data Center as CCDC-778816−778819. These data can be obtained free of charge from The Cambridge Crystallographic Data Centre via www.ccdc.cam.ac.uk/data_request/cif and are also available as Supporting Information.

Acknowledgment. This work was financially supported by the Deutsche Forschungsgemeinschaft.

Supporting Information Available: Computational details (PDF) and X-ray crystallographic data (CIF). This material is available free of charge via the Internet at http://pubs.acs.org.

JA1049548